Electronic Supplementary Information (ESI) for

Switching between Porphyrin, Porphodimethene and Porphyrinogen using Cyanide and Fluoride ions mimicking Volatile Molecular Memory and 'NOR' Logic Gate

Mandeep K. Chahal and Muniappan Sankar

Department of Chemistry, Indian Institute of Technology Roorkee, Roorkee-247667, India

Table of Contents

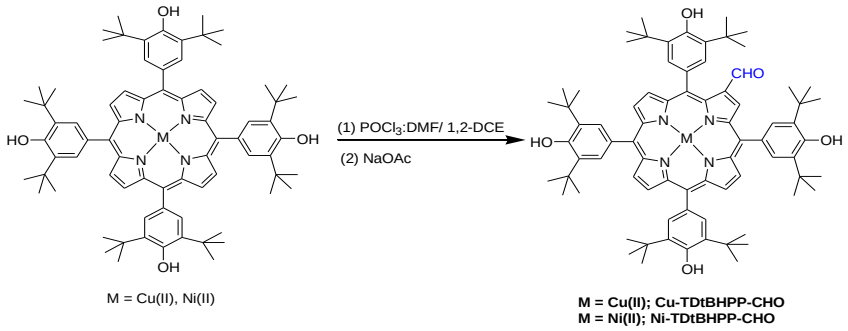

Scheme S1. Multigram scale preparation of β-formyl substituted porphyrins.

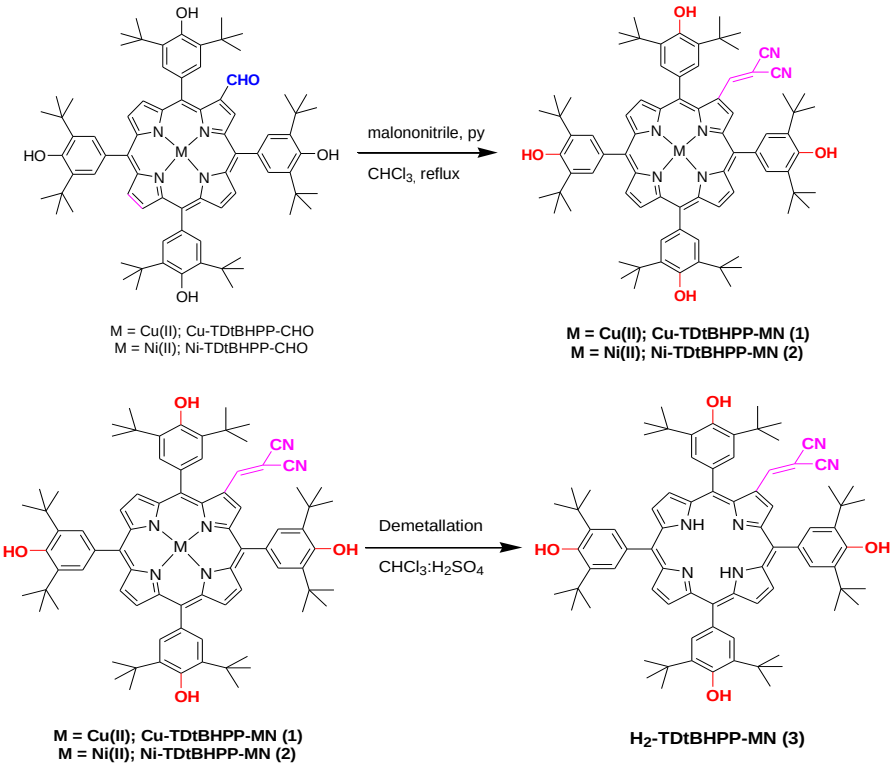

Scheme S2. Synthetic procedure for targeted porphyrins **1**, **2** and **3**.

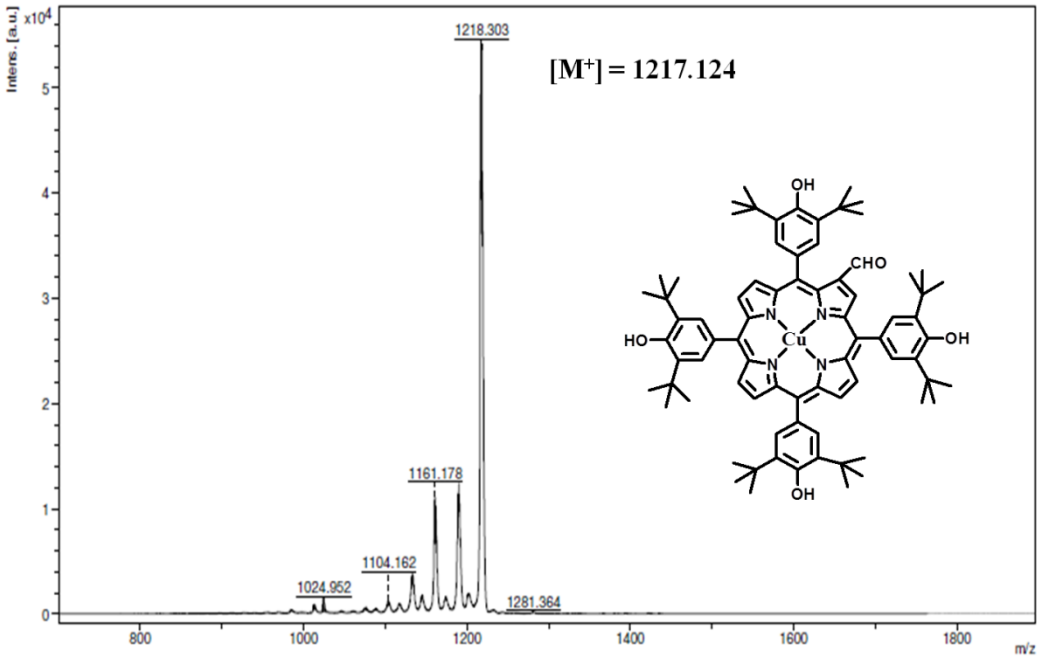

Figure S1. MALDI-TOF mass spectrum of Cu-TDtBHPP-CHO**.**

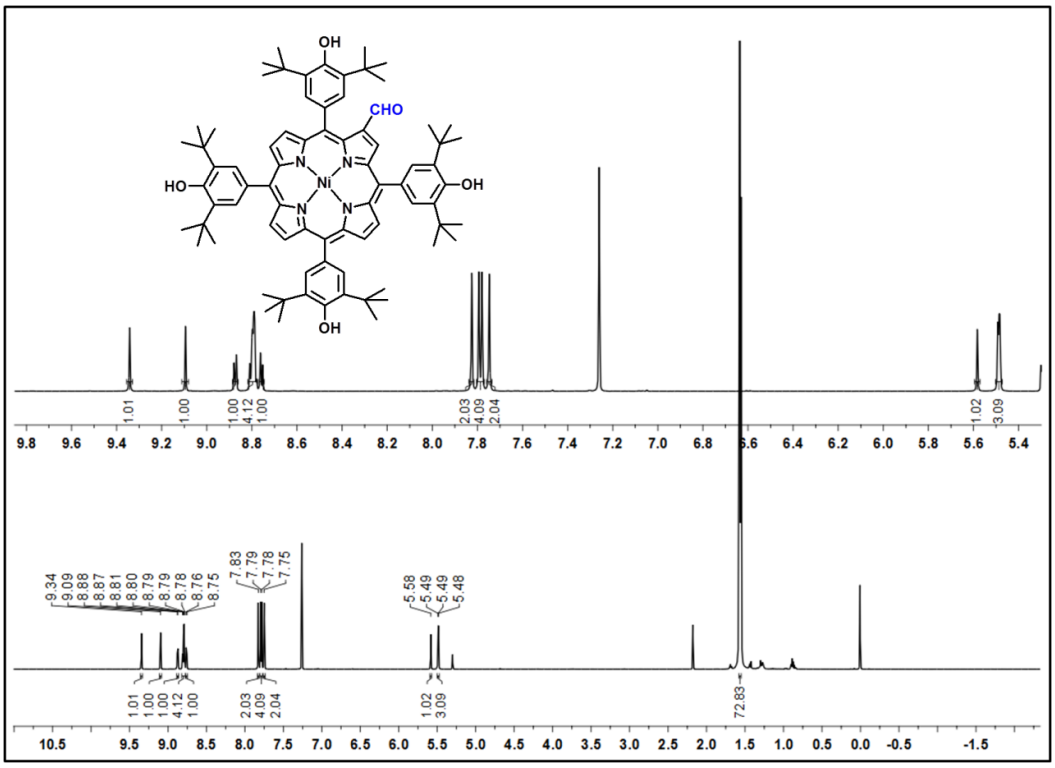

Figure S2. ^{1}H NMR spectrum of Ni-TDtBHPP-CHO.

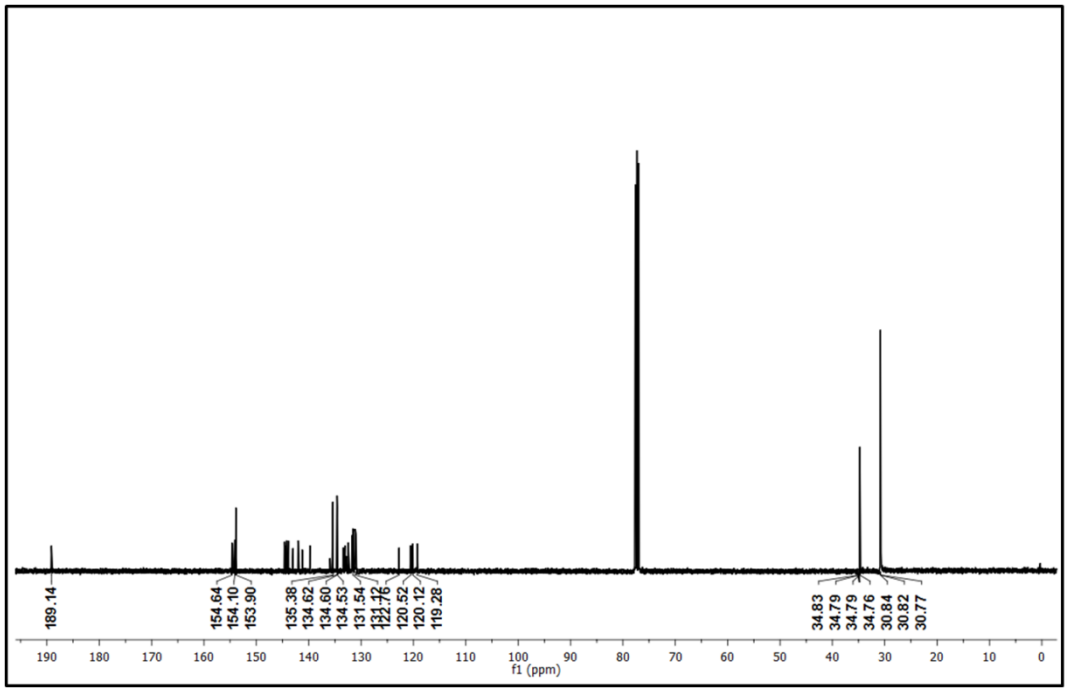

Figure S3. ^{13}C NMR spectrum of Ni-TDtBHPP-CHO.

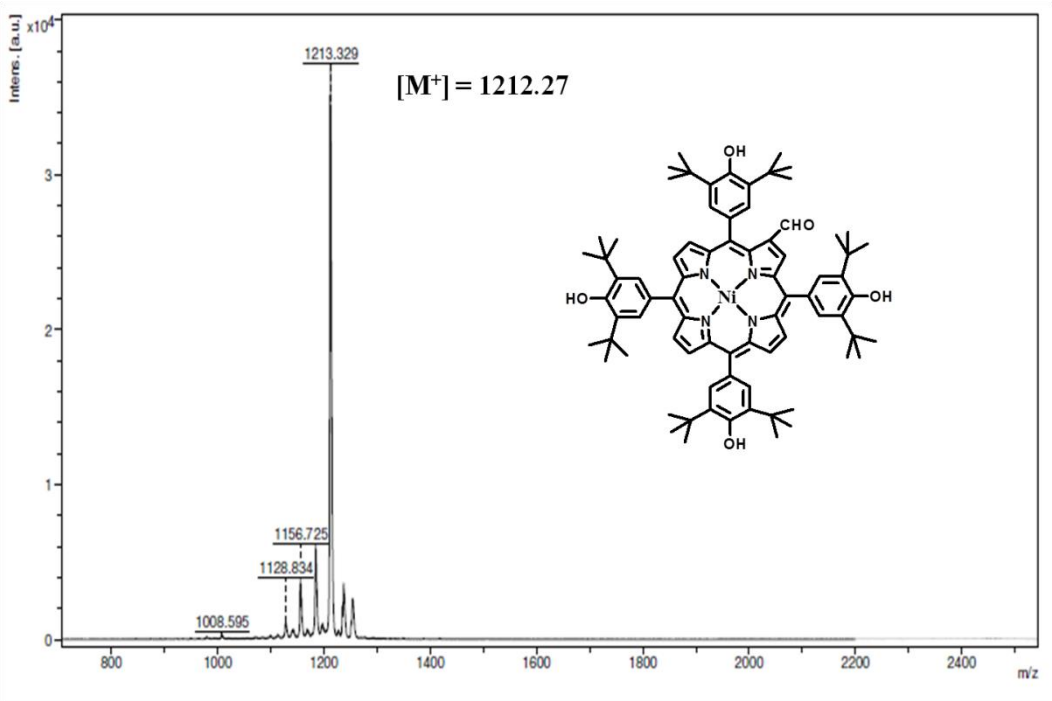

Figure S4. MALDI-TOF mass spectrum of Ni-TDtBHPP-CHO.

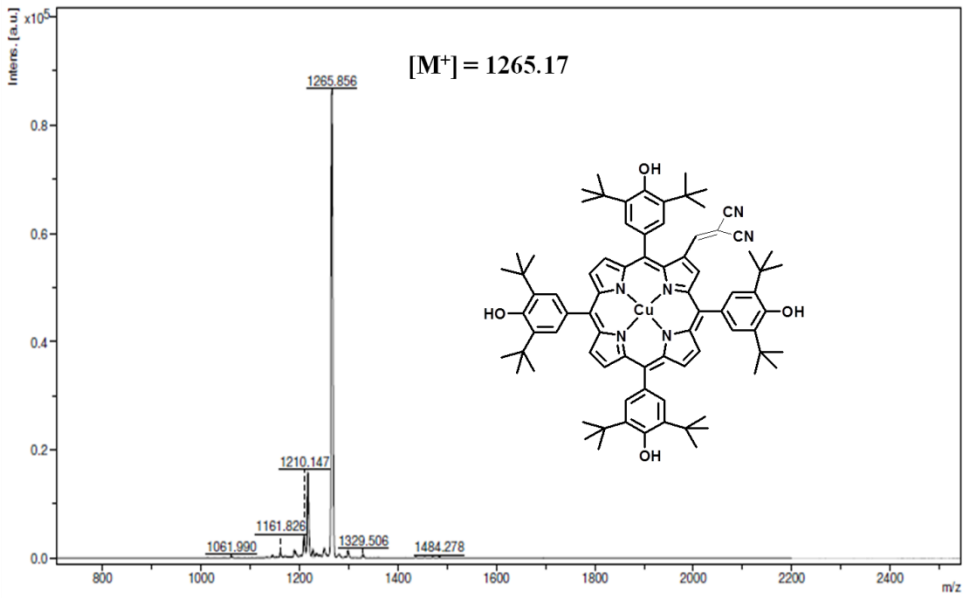

Figure S5. MALDI-TOF mass spectrum of Cu-TDtBHPP-MN (**1**).

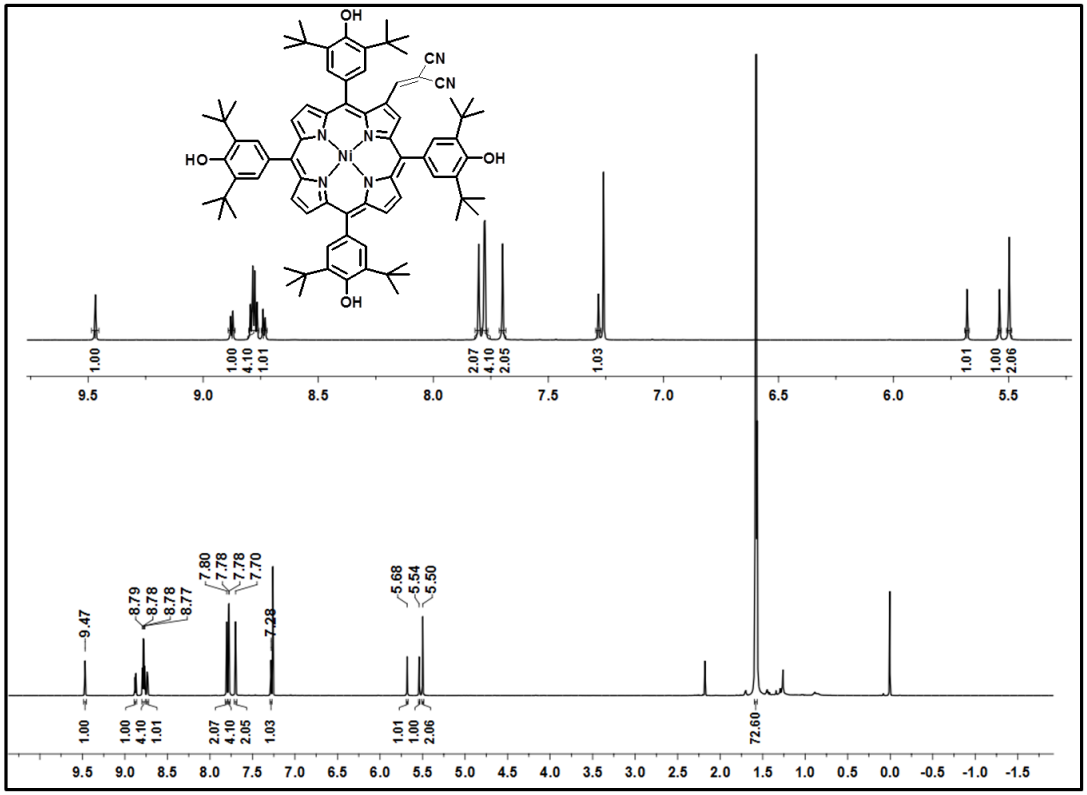

Figure S6. ^{1}H NMR spectrum of Ni-TDtBHPP-MN (**2**).

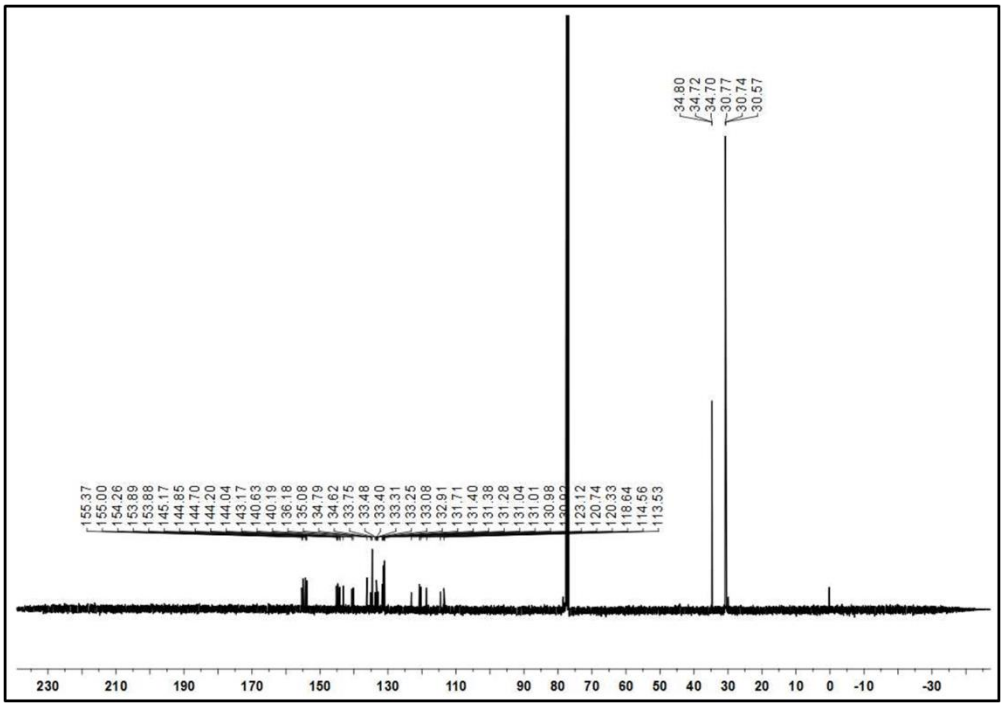

Figure S7. ^{13}C NMR spectrum of Ni-TDtBHPP-MN (**2**).

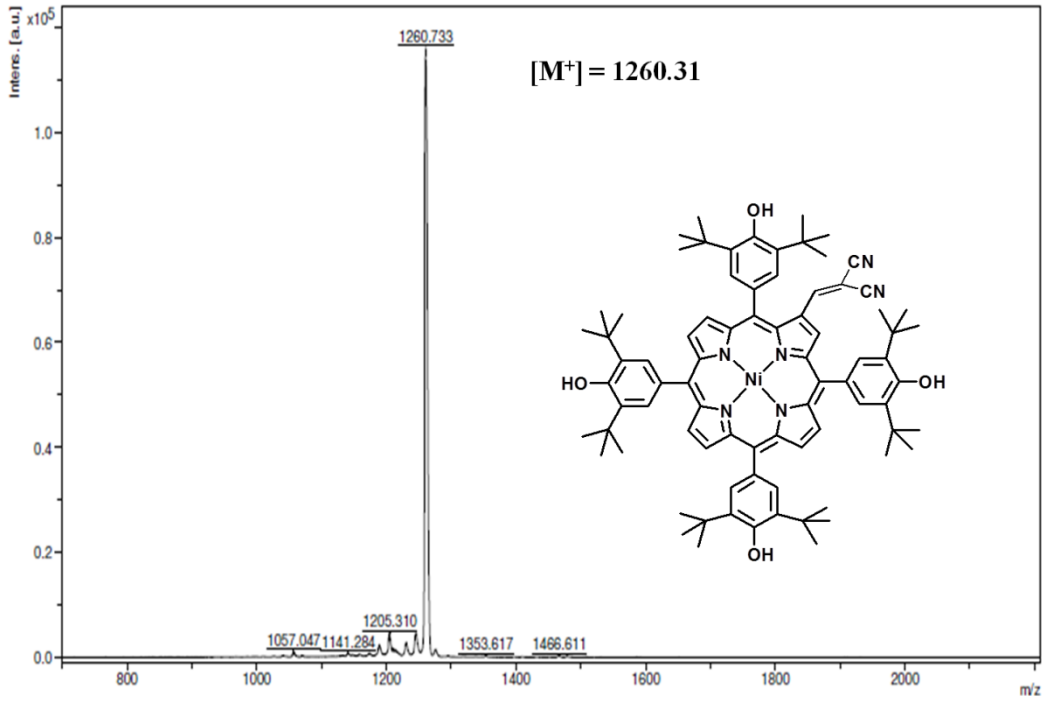

Figure S8. MALDI-TOF mass spectrum of Ni-TDtBHPP-MN (**2**).

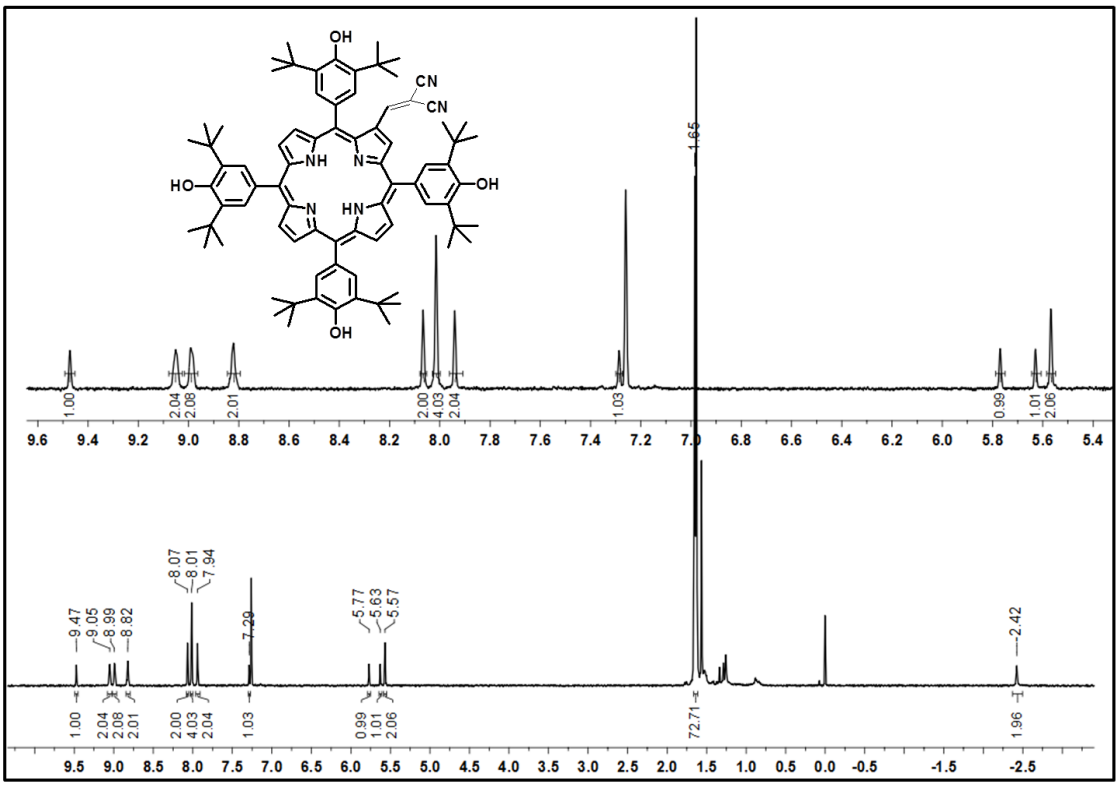

Figure S9. ^{1}H NMR spectrum of H_2-TDtBHPP-MN (**3**).

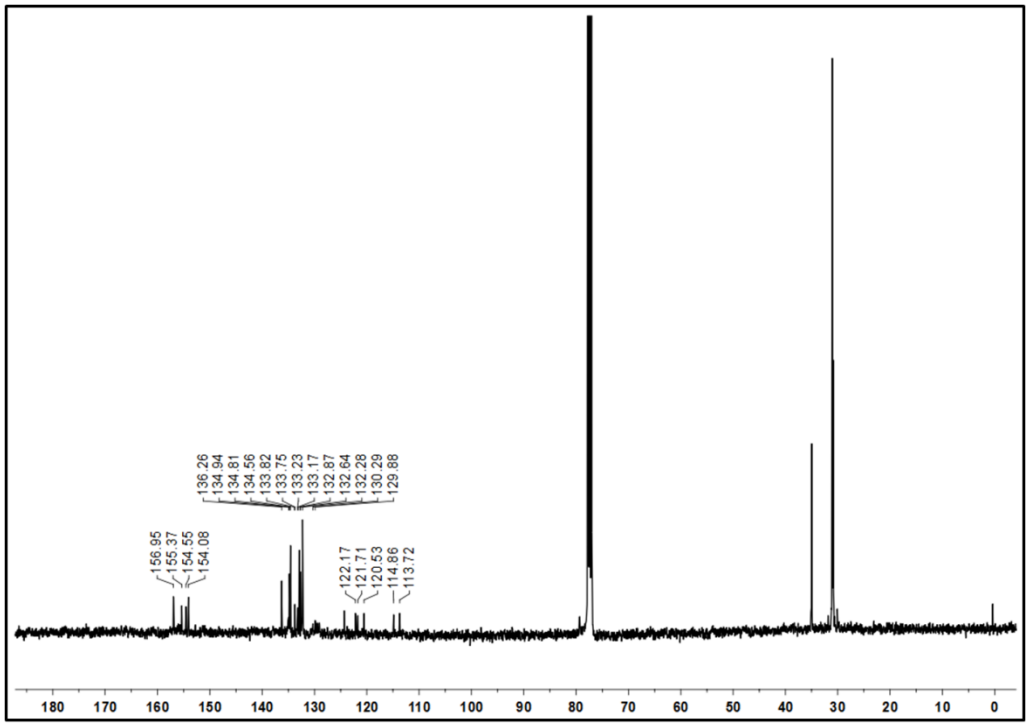

Figure S10. ^{13}C NMR spectrum of H_2-TDtBHPP-MN (**3**).

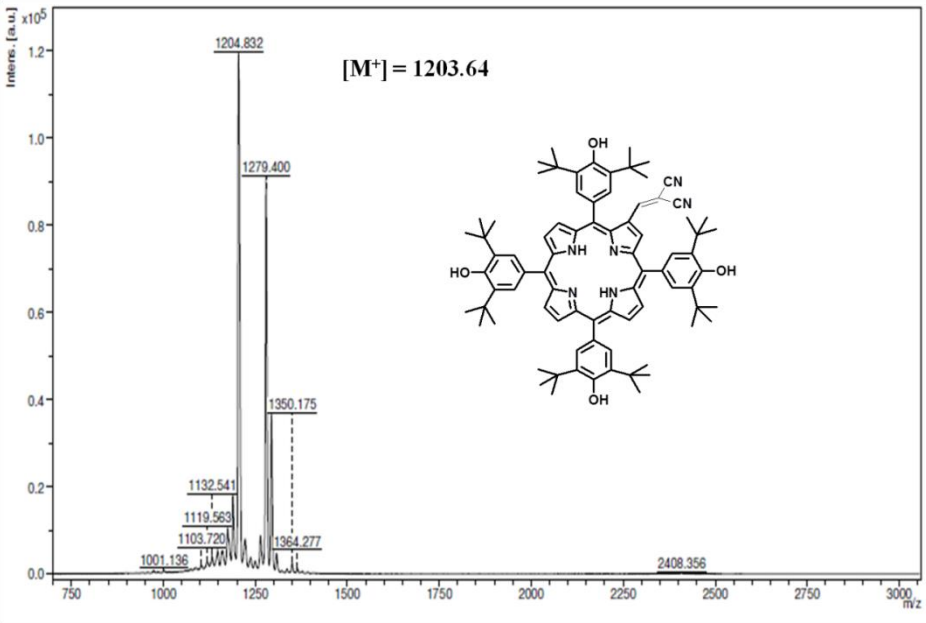

Figure S11. MALDI-TOF mass spectrum of H_2-TDtBHPP-MN (**3**).

Table S1. Crystal data of Cu-TDtBHPP-CHO	
Empirical formula	$C_{83}H_{105}N_4O_5Cu$
Formula Weight	1303.26
Crystal system	Triclinic
Space group	P-1
a (Å)	10.8479(4)
b (Å)	14.6207(5)
c (Å)	15.9745(5)
α (°)	70.078(2)
β (°)	76.389(2)
γ (°)	68.533(2)
Volume ($Å^3$)	2198.97(13)
Z	1
D_{cald} (g/cm^3)	0.984
Wavelength	0.71073
Temperature (K)	296 K
No. of total reflections	10936
No. of independent reflections	6457
R^a	0.0568
$R_w{}^b$	0.1609
CCDC	1451709

Table S2. Optical absorption spectral data of synthesized porphyrins in CH_2Cl_2 at 298 K.

Porphyrin	B band(s), nm	Q band(s), nm
Ni-TDtBHPP	422	532
Cu-TDtBHPP	422	542, 581
H_2-TDtBHPP	425	522,559,596,652
Ni-TDtBHPP-CHO	436	545,586
Cu-TDtBHPP-CHO	435	555,598
Ni-TDtBHPP-MN **(2)**	393,462	554,613
Cu-TDtBHPP-MN **(1)**	400,462	563,618
H_2-TDtBHPP-MN **(3)**	415,464	541,625,689

Table S3. Electrochemical Redox Data (vs Ag/AgCl) of synthesized porphyrins in CH_2Cl_2 containing 0.1 M $TBAPF_6$ at 298 K. Scan rate 0.1 Vs^{-1}.

Porphyrin	Oxidation(V)		$\Delta E_{1/2}$(V)	Reduction(V)	
	I	II		I	II
Ni-TDtBHPP	0.87[a]		2.24	-1.370[a]	
Cu-TDtBHPP	0.76		2.19	-1.430	
Cu-TDtBHPP-CHO	0.82	1.16	2.04	-1.220	-1.590
Ni-TDtBHPP-CHO	0.933		2.122	-1.189	-1.323
Cu-TDtBHPP-MN (**1**)	0.864	1.242	1.850	-0.987	-1.300
Ni-TDtBHPP-MN (**2**)	0.975		1.949	-0.974	-1.150
H_2-TDtBHPP-MN (**3**)	0.989		1.878	-0.889	

$\Delta E_{1/2} = I_{oxd.} - I_{red.}$. Pt working and Pt wire counter electrodes were used. [a]Data taken from DPV.

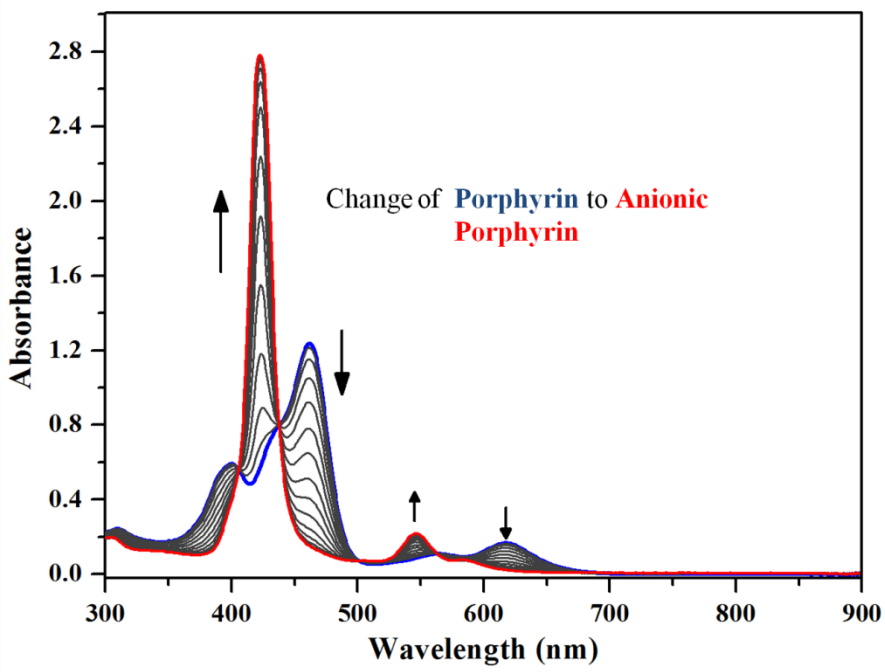

Figure S12. UV/Vis titration of CN^- (0 - 9.32×10^{-5} M) to Cu-TDtBHPP-MN **(1)** (8 μM).

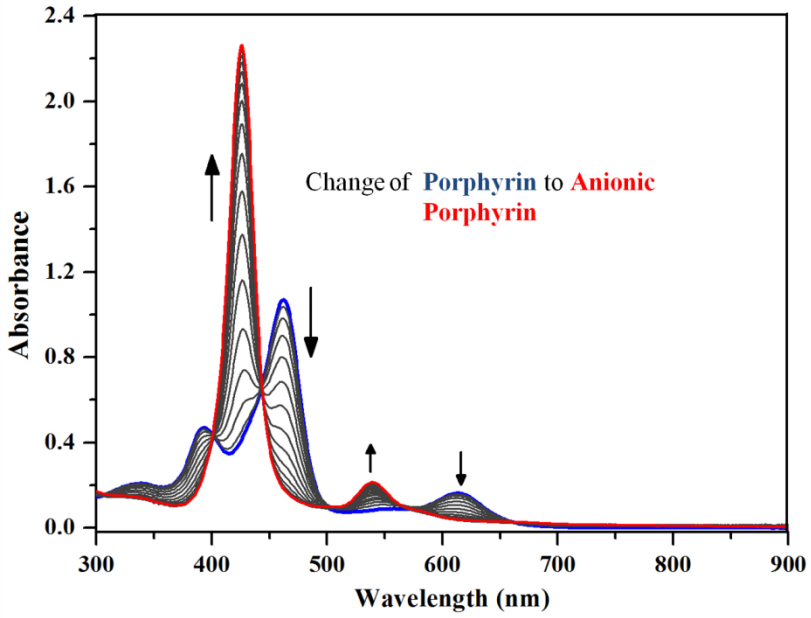

Figure S13. UV/Vis titration of CN^- (0 - 9.32×10^{-5} M) to Ni-TDtBHPP-MN **(2)** (8 μM).

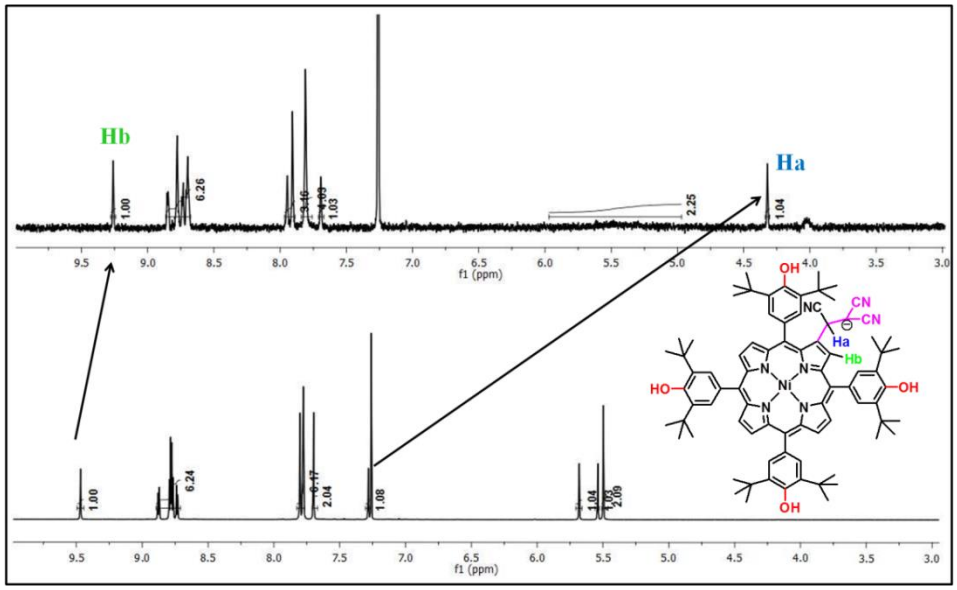

Figure S14. ^{1}H NMR spectra of the adduct **[2·CN]**$^{-}$ after addition of CN^{-} ions (1 equiv.) to Ni-TDtBHPP-MN (**2**) (5×10^{-3} M) in $CDCl_3$ at 298 K.

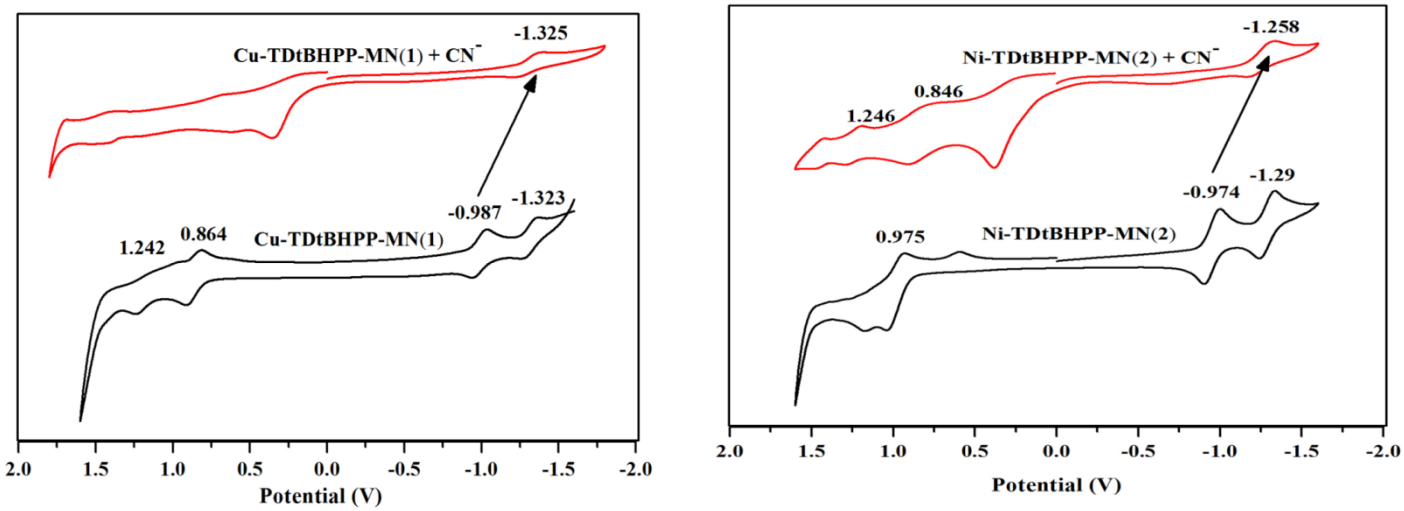

Figure S15. Cyclic voltammetric traces of Cu-TDtBHPP-MN **(1)** (left) and Ni-TDtBHPP-MN(**2**) (right) in absence and presence of CN^{-} ions containing 0.1 M $TBAPF_6$ at 298 K.

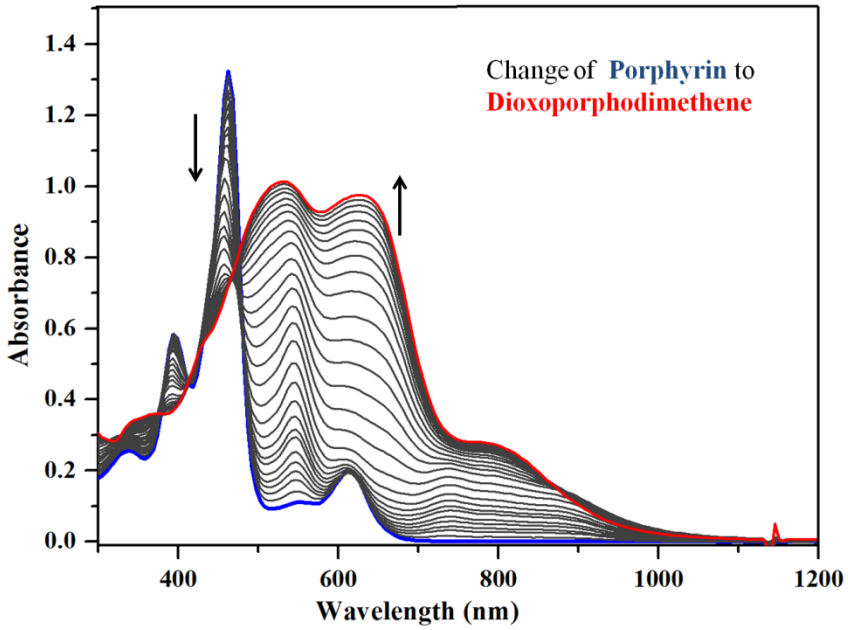

Figure S16. UV/Vis titration of F^- (0–10^{-3} M) to Ni-TDtBHPP-MN **(2)** (8 μM) changing porphyrin to porphodimethene.

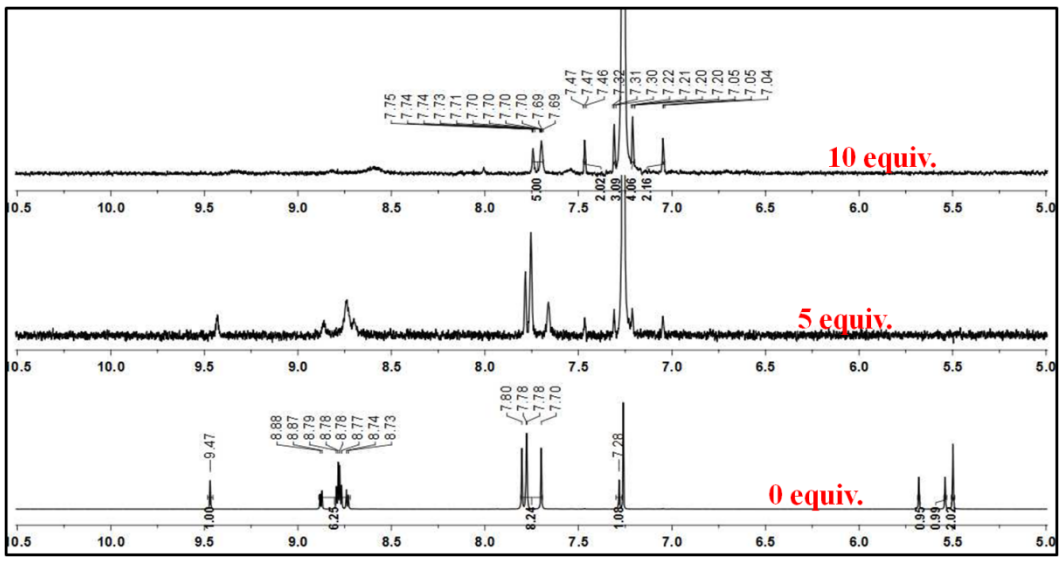

Figure S17. ^{1}H NMR spectra of **2** with increasing concentration of F^- ions (0-10 equiv.) in $CDCl_3$, 500 MHz.

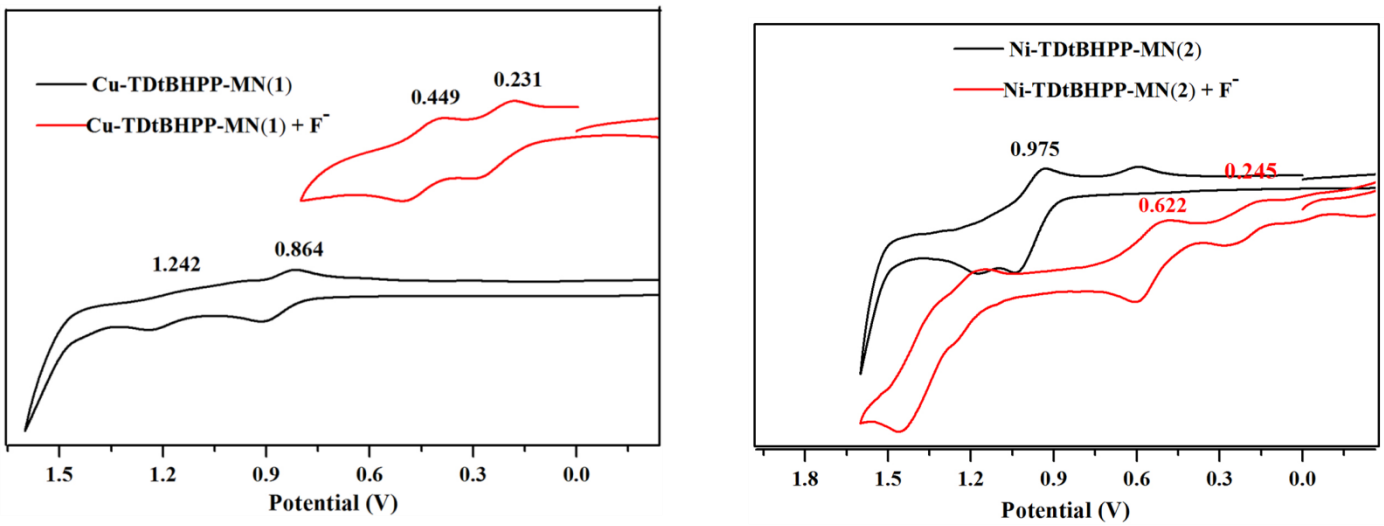

Figure S18. Cyclic voltammetric traces of Cu-TDtBHPP-MN **(1)** (left) and Ni-TDtBHPP-MN (**2**) (right) in absence and presence of F^- ions containing 0.1 M $TBAPF_6$ at 298 K.

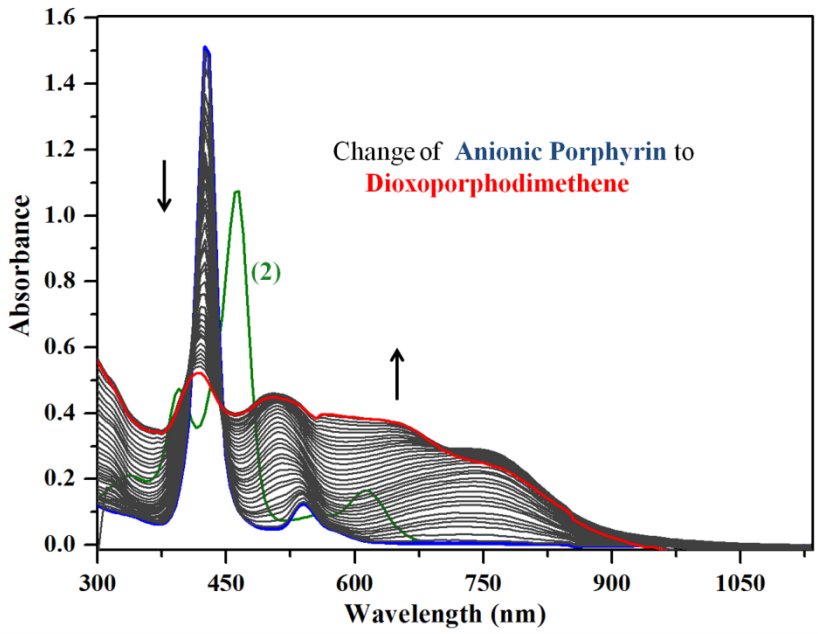

Figure S19. UV/Vis titration of F^- (0–4X10^{-3} M) to (Ni-TDtBHPP-MN + CN^-) (6 μM) changing anionic porphyrin to anionic porphodimethene.

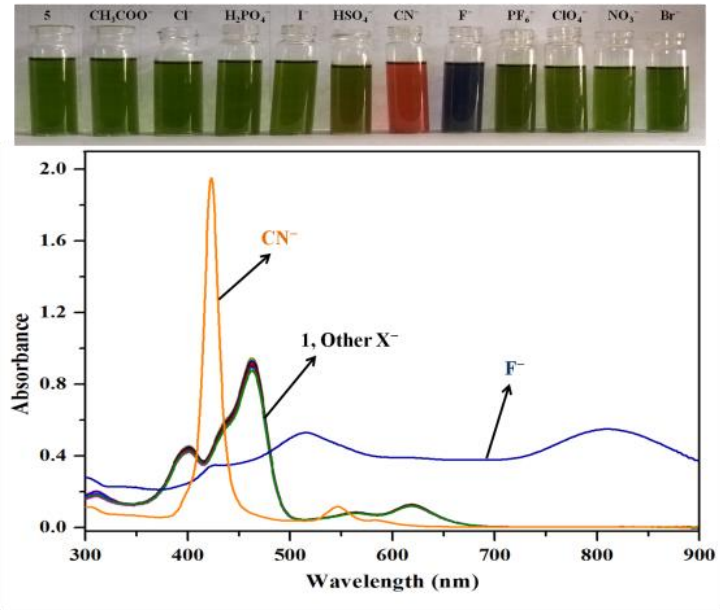

Figure S20. Absorption spectra and colorimetric changes for Cu-TDtBHPP-MN **(1)** (8 μM) in the presence of different anions. Changes observed only for F^- and CN^- ions.

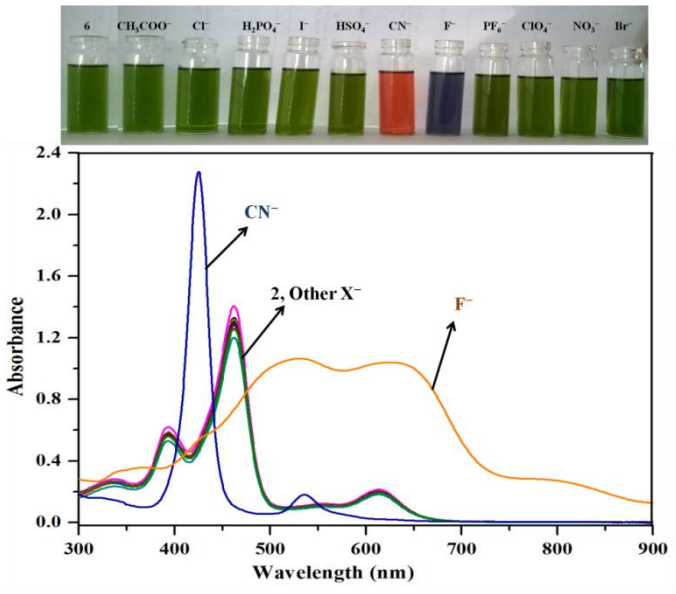

Figure S21. Absorption spectra and colorimetric changes for Ni-TDtBHPP-MN **(2)** (8 μM) in the presence of different anions. Changes observed only for F^- and CN^- ions.

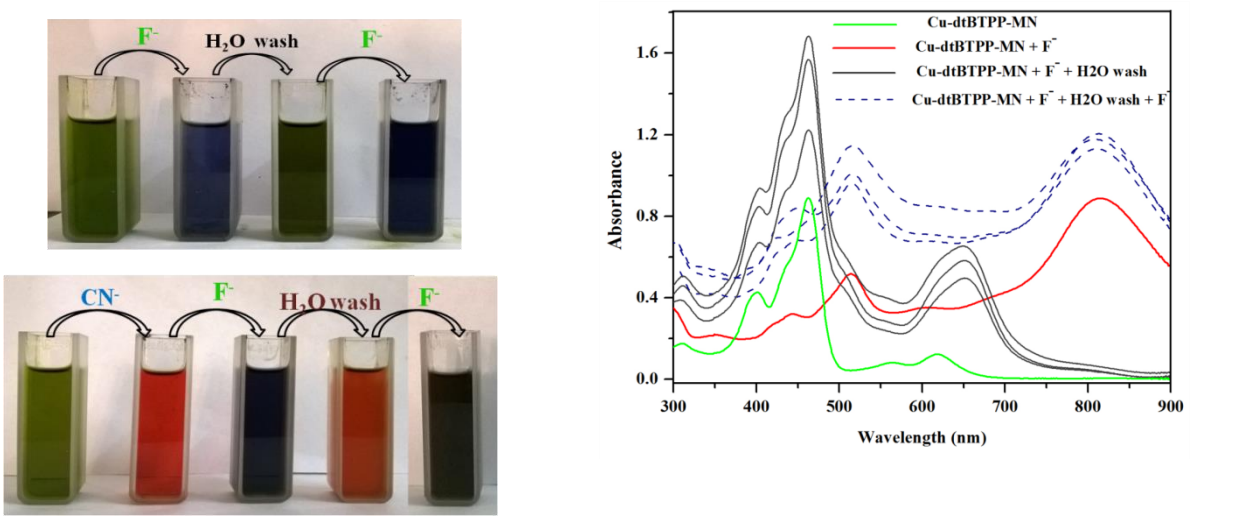

Figure S22. Visual response for reversibility for F⁻ ions (left) and UV/Vis response for reversibility for F⁻ ions in case of **1** (right) (metalloporphyrin spectrum regenerated with marginal shift in Qx(0,0) band)**.**

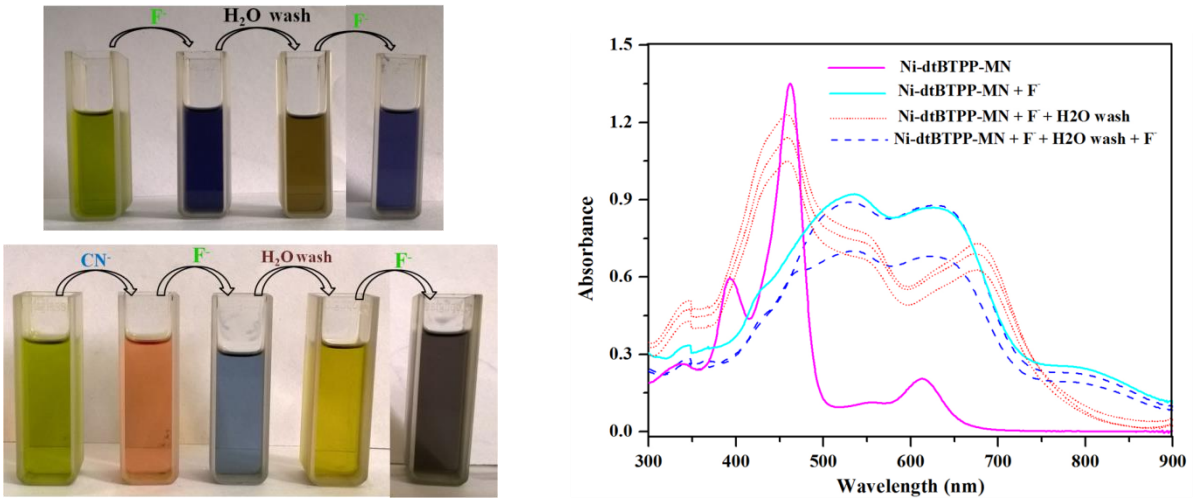

Figure S23. Visual response for reversibility for F⁻ ions (left) and UV/Vis response for reversibility for F⁻ ions in case of **2** (right) (distortion in Q bands are more probably due to autoxidation)**.**

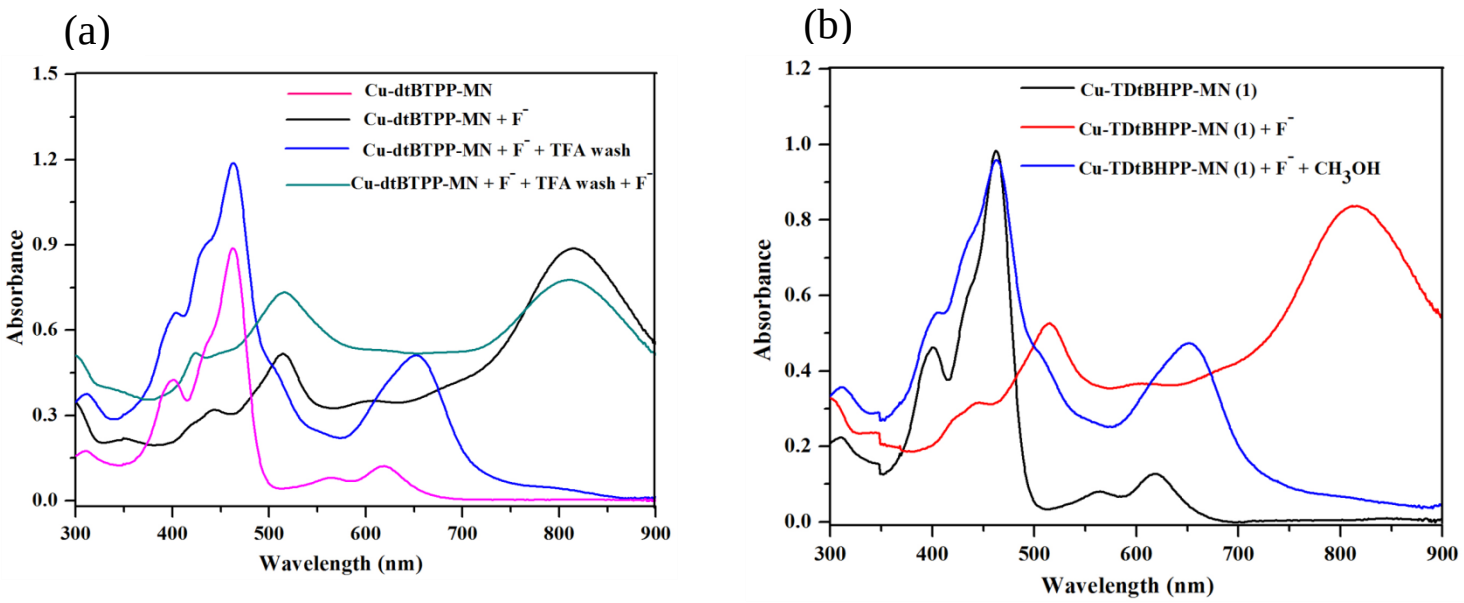

Figure S24. (a) UV/Vis response for reversibility for F^- ions using trifluoroacetic acid (TFA) in case of Cu-TDtBHPP-MN (**1**). (b) UV/Vis response for reversibility for F^- ions using CH_3OH in case of Cu-TDtBHPP-MN (**1**).

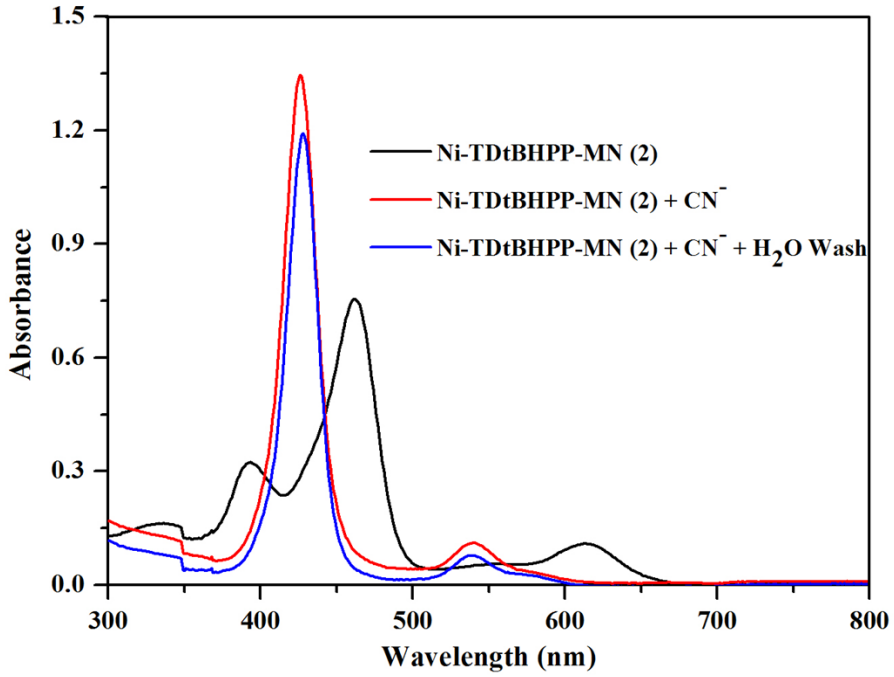

Figure S25. Effect of water on anionic porphyrin formed after the addition of cyanide ions to Ni-TDtBHPP-MN (**2**).

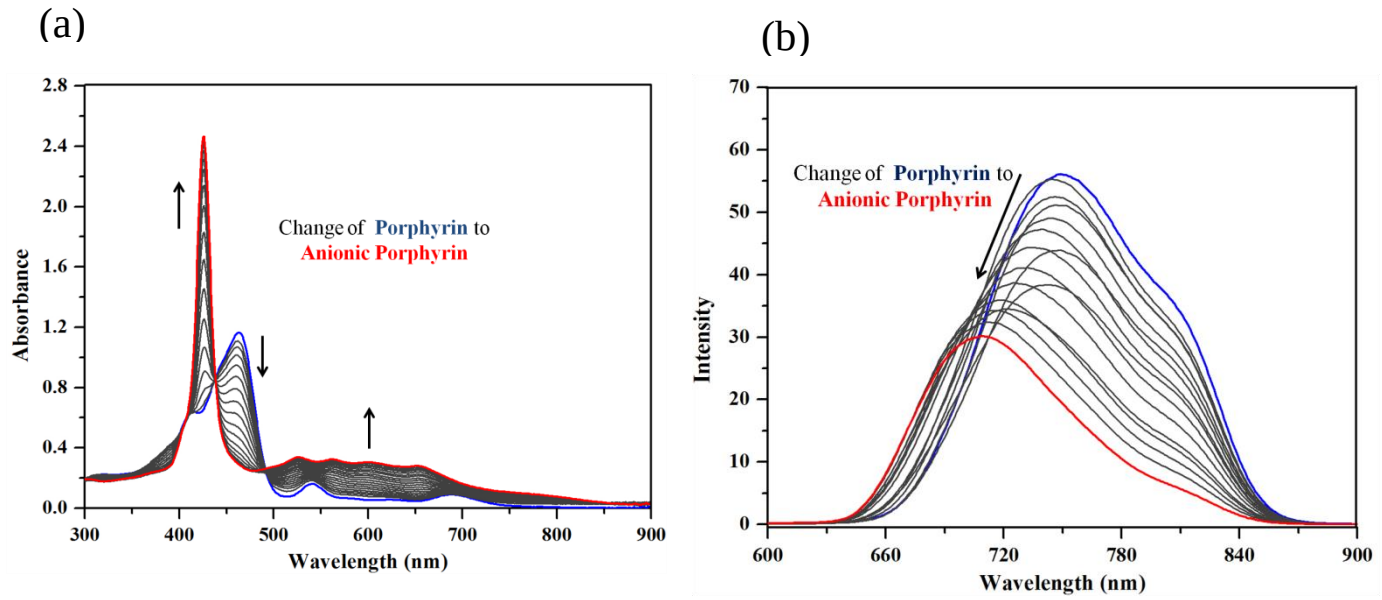

Figure S26. (a) Electronic absorbance changes upon addition of CN^- (0-2.5x10^{-4}M) (b) Fluorescence emission intensity changes upon addition of CN^- (0-2x10^{-4}M) into **3** in CH_2Cl_2 (conversion of porphyrin to anionic porphyrin).

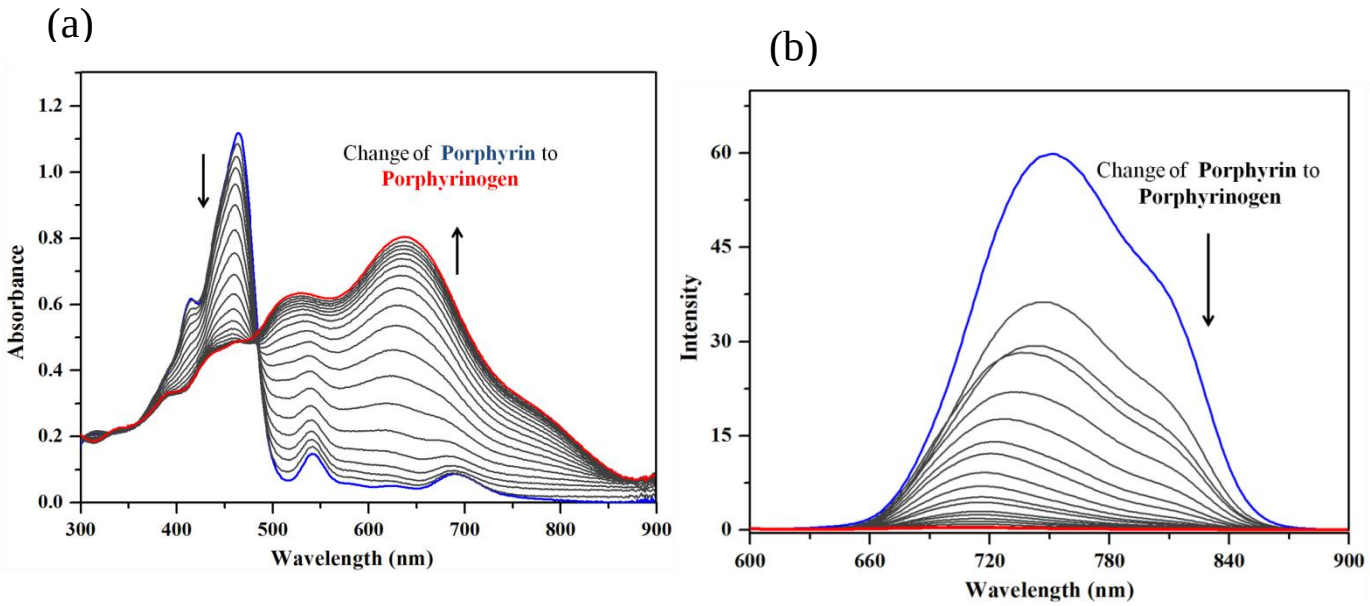

Figure S27. (a) Electronic absorbance changes upon addition of F^- (0-9.5x10^{-4}M) and (b) fluorescence emission intensity changes upon addition of F^- (0-8.5x10^{-4}M) into **3** in CH_2Cl_2 (conversion of porphyrin to porphyrinogen).

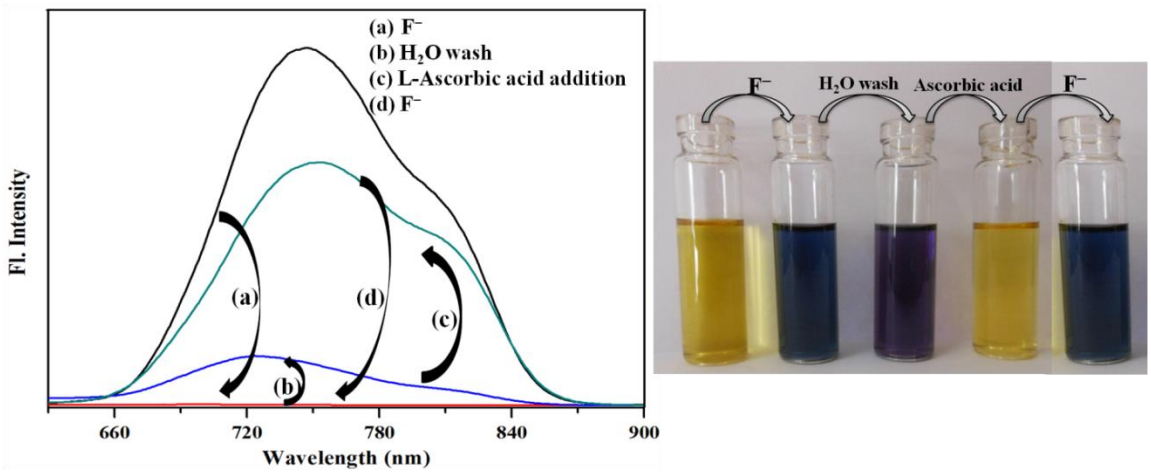

Figure S28. Fluorescence emission intensity changes of **3** for reversibility and reusability tests with F^- ions (left) and their corresponding colorimetric response (right).

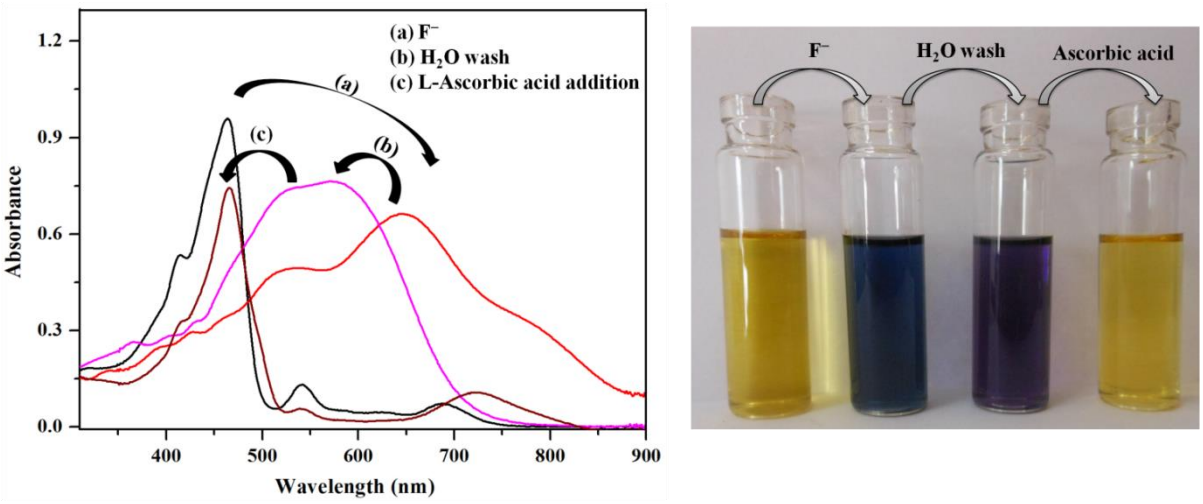

Figure S29. UV-Visible spectral changes of **3** for reversibility and reusability tests with F^- ions (left) and their corresponding colorimetric response (right).

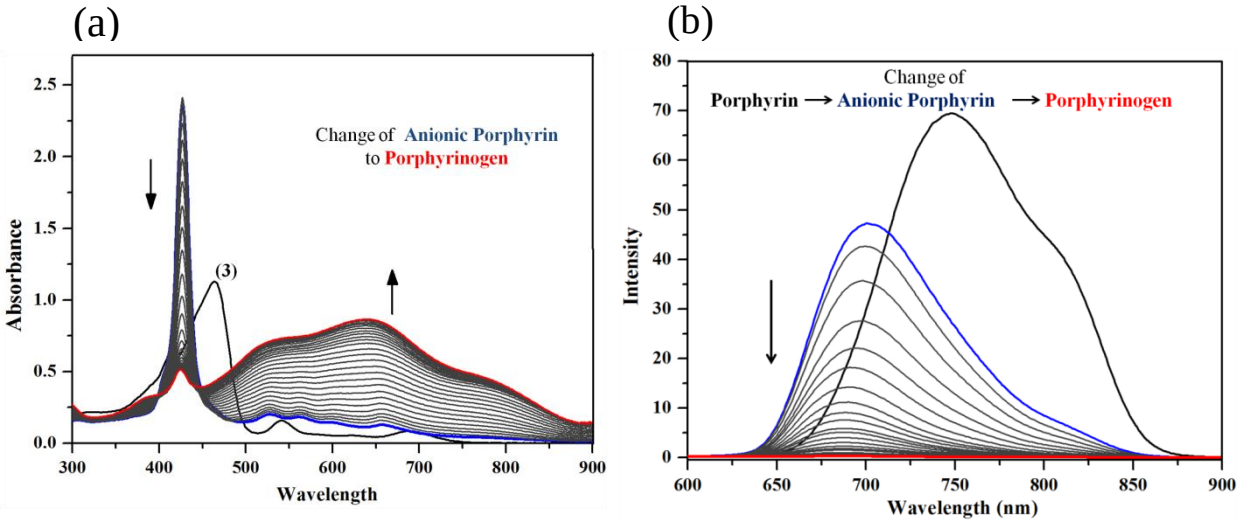

Figure S30. (a) Electronic absorbance changes of **5** upon addition of F^- (0-2.5x10^{-3}M) and (b) Fluorescence emission intensity changes upon addition of F^- (0-2x10^{-3}M) into **5** in CH_2Cl_2 (conversion of anionic porphyrin to anionic porphyrinogen).

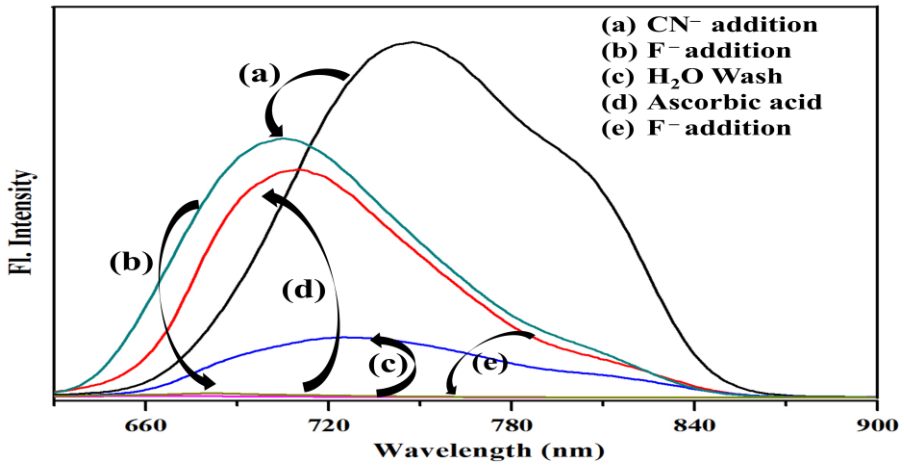

Figure S31. Fluorescence emission intensity changes of **5** with F^- ion.

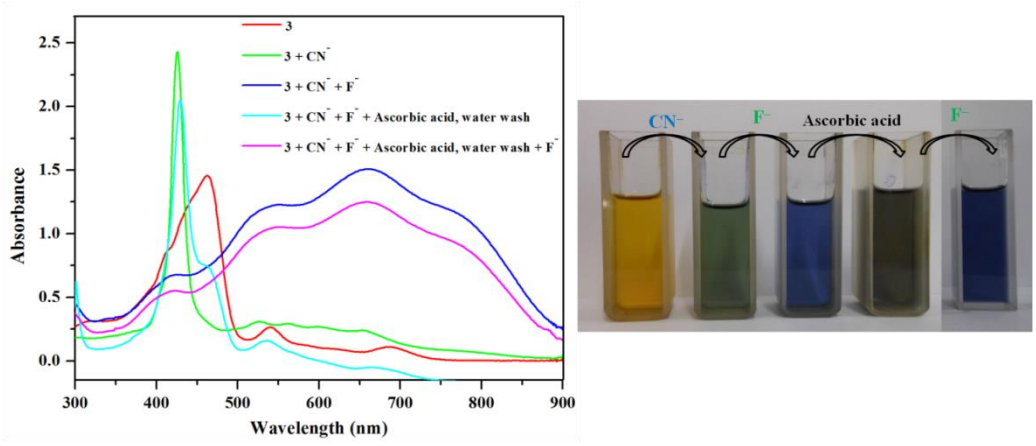

Figure S32. UV-Visible spectral changes of **5** for reversibility and reusability tests with F^- ions using L-ascorbic acid (left) and their corresponding colorimetric response (right).

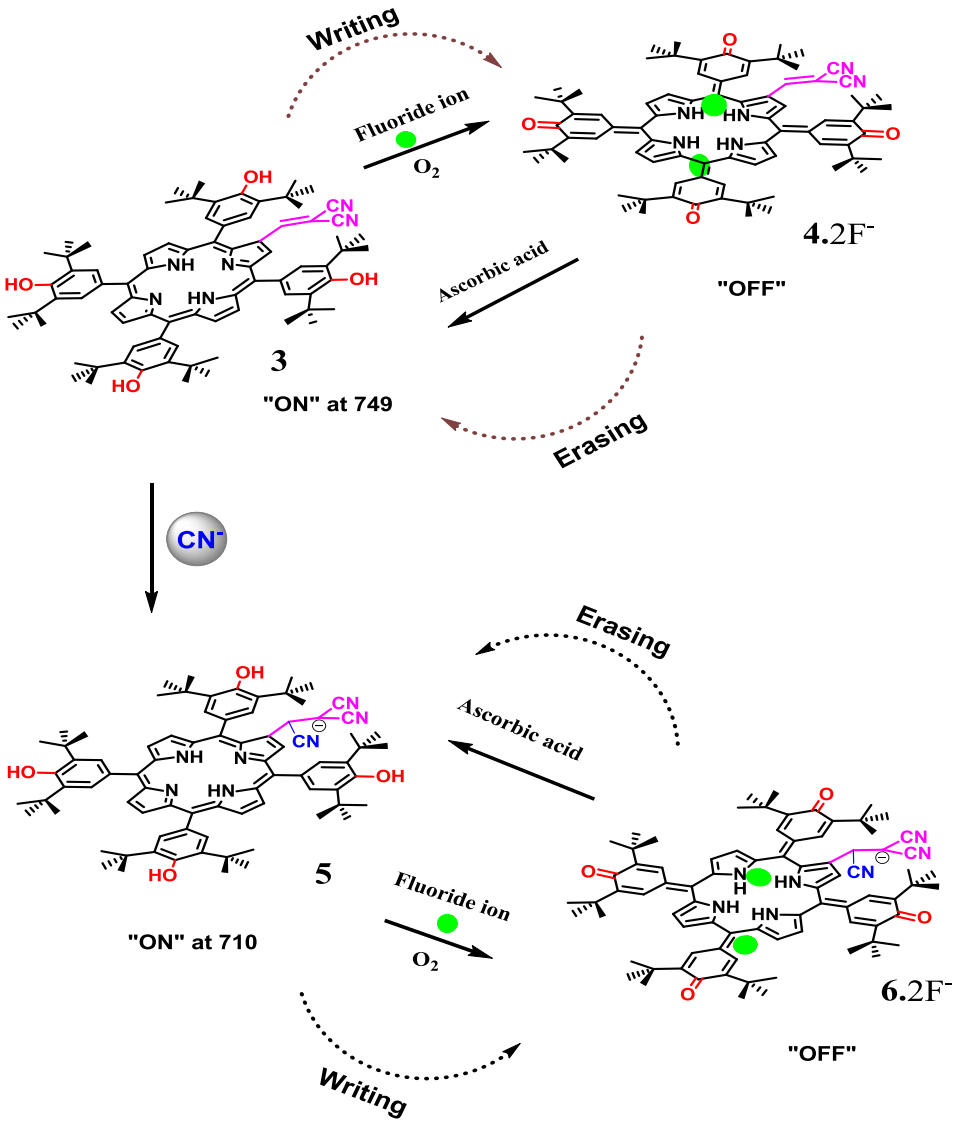

Figure S33. The "writing–erasing" cycle of **3** and **5**.

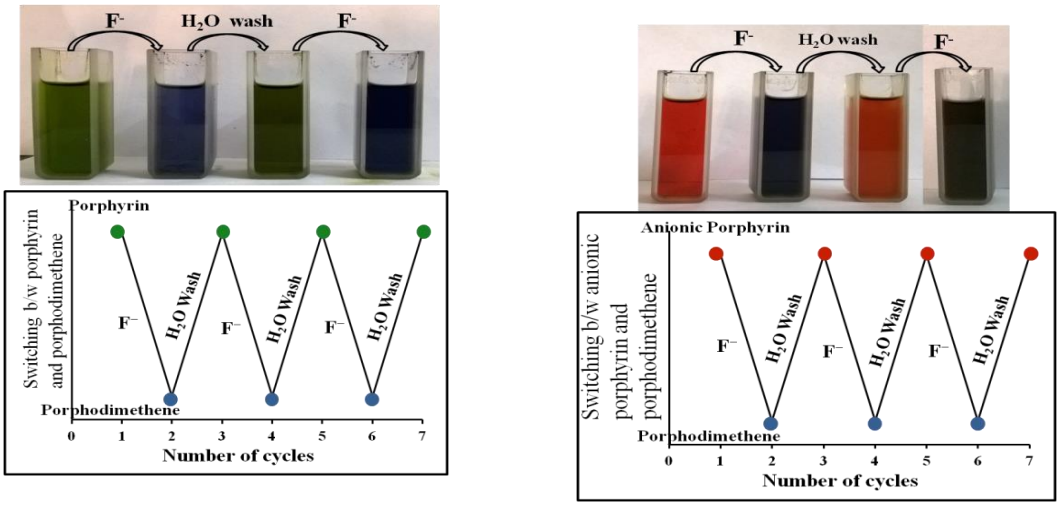

Figure S34. Repeated memory cycles using **1A** (left) and **1B** (right) in which one state was detected by the absorbance for porphyrin and other state by the absorbance for porphodimethene in CH_2Cl_2 for Cu-TDtBHPP-MN (**1**). Photographs showed the colour of each state under 'naked-eye'.

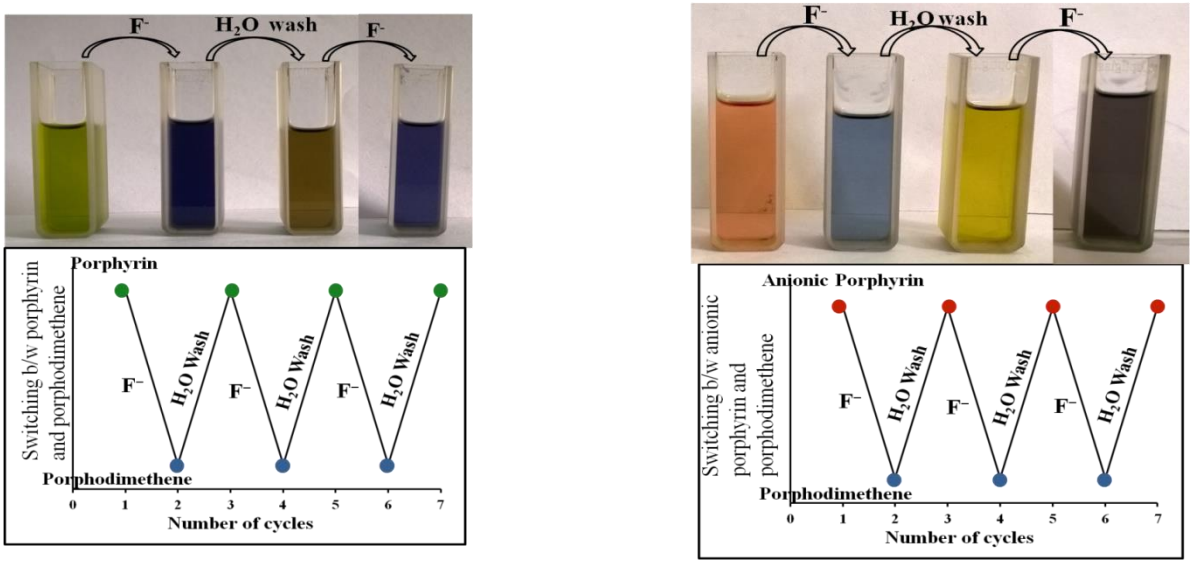

Figure S35. Repeated memory cycles using **1A** (left) and **1B** (right) in which one state was detected by the absorbance for porphyrin and other state by the absorbance for porphodimethene in CH_2Cl_2 for Ni-TDtBHPP-MN (**2**). Photographs showed the colour of each state under 'naked-eye'.

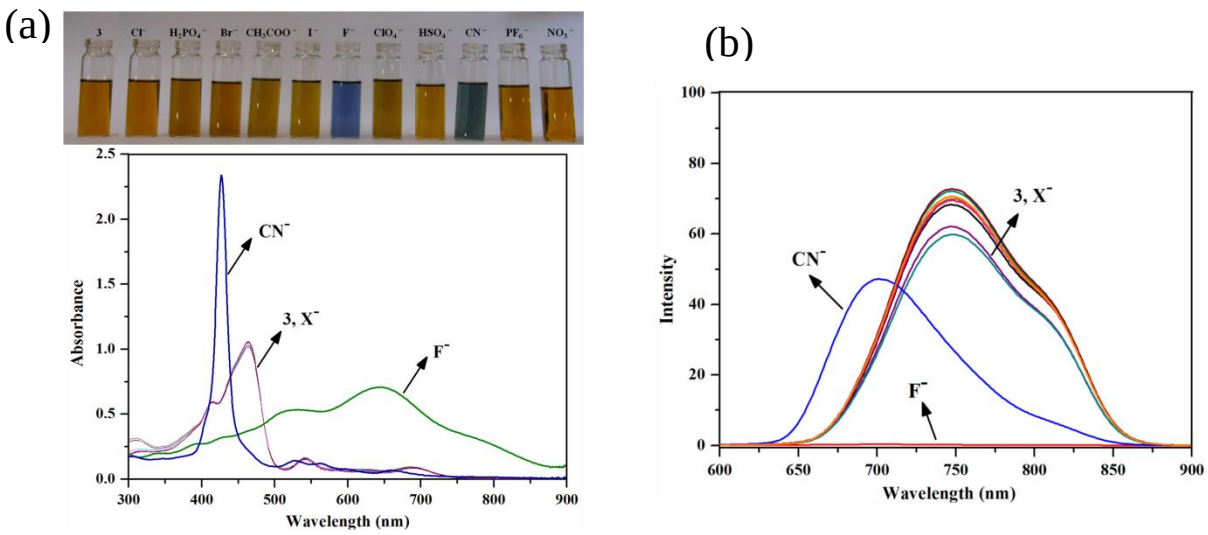

Figure S36. (a) Electronic absorbance and (b) fluorescence emission intensity changes upon addition of 10 equivalents of different tetra-*n*-butylammonium salts into CH_2Cl_2 solution of **3**.

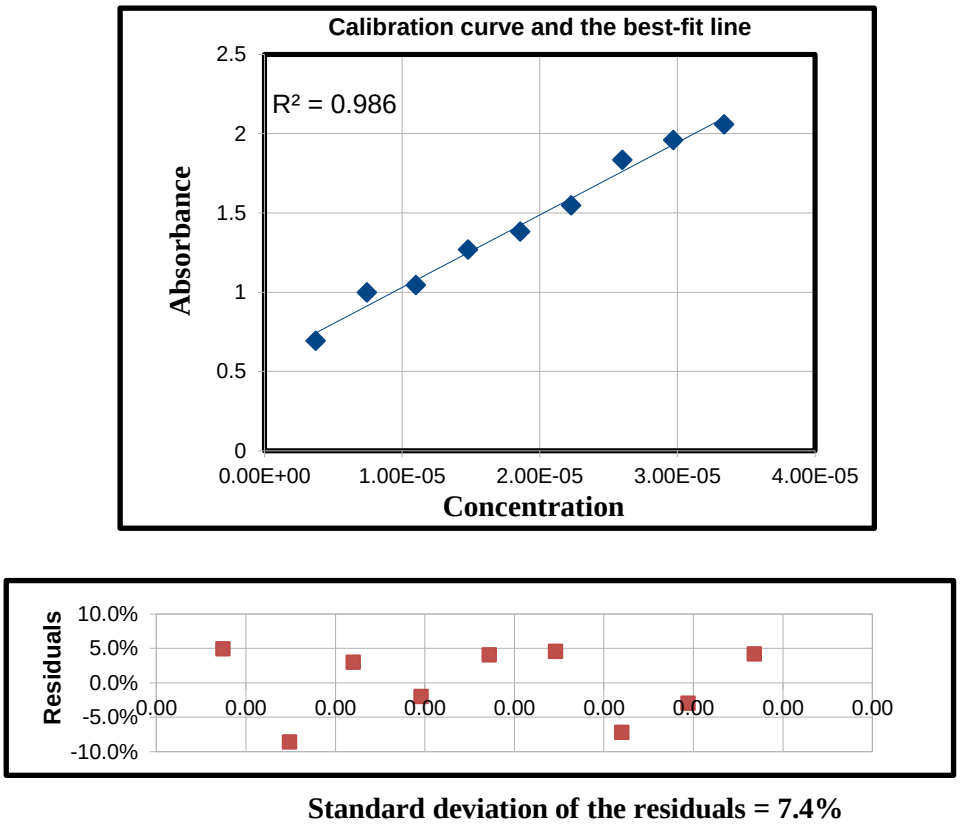

	Value	Error (σ)	% Error
Slope	1123.9013	58.9624	5.25%
Intercept	0.0626	0.0157	25.16%

Figure S37. Analytical calibration curve using a simple liner curve fit, with error estimation of Cu-TDtBHPP-MN (**1**) for fluoride addition.

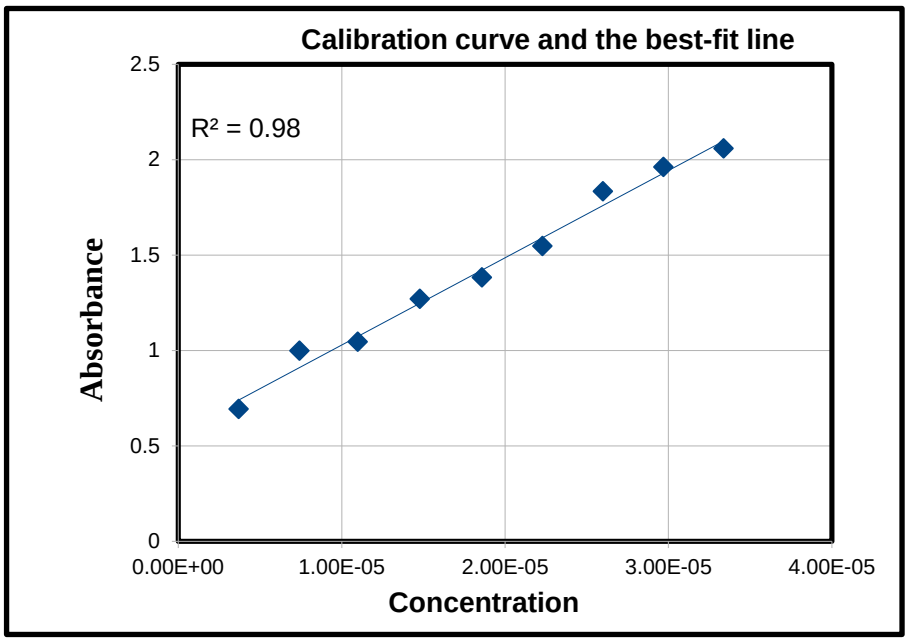

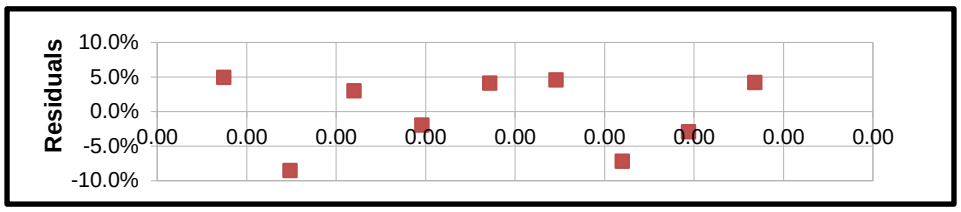

Standard deviation of the residuals = 6.7%

	Value	Error (σ)	% Error
Slope	66352.4460	3134.4887	4.72%
Intercept	0.3526	0.0655	18.57%

Figure S38. Analytical calibration curve using a simple liner curve fit, with error estimation of Cu-TDtBHPP-MN (**1**) for cyanide addition.

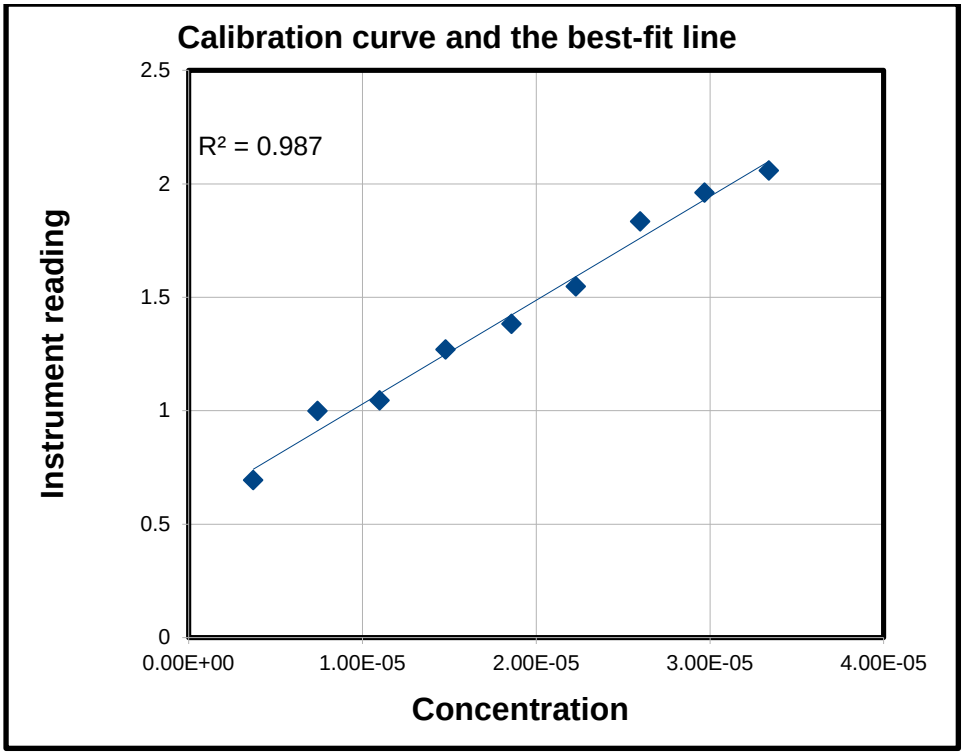

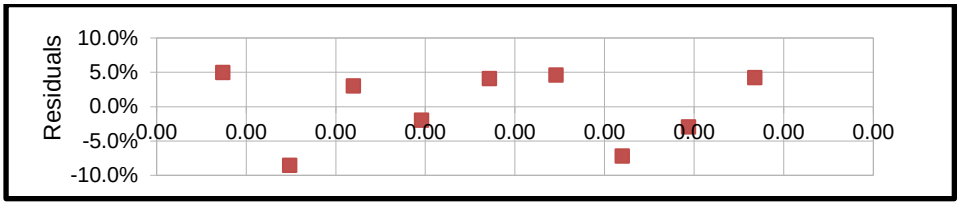

Standard deviation of the residuals = 4.8%

	Value	Error (σ)	% Error
Slope	45748.3802	1974.8304	4.32%
Intercept	0.5720	0.0412	7.21%

Figure S39. Analytical calibration curve using a simple liner curve fit, with error estimation of H_2-TDtBHPP-MN (**3**) for cyanide addition.

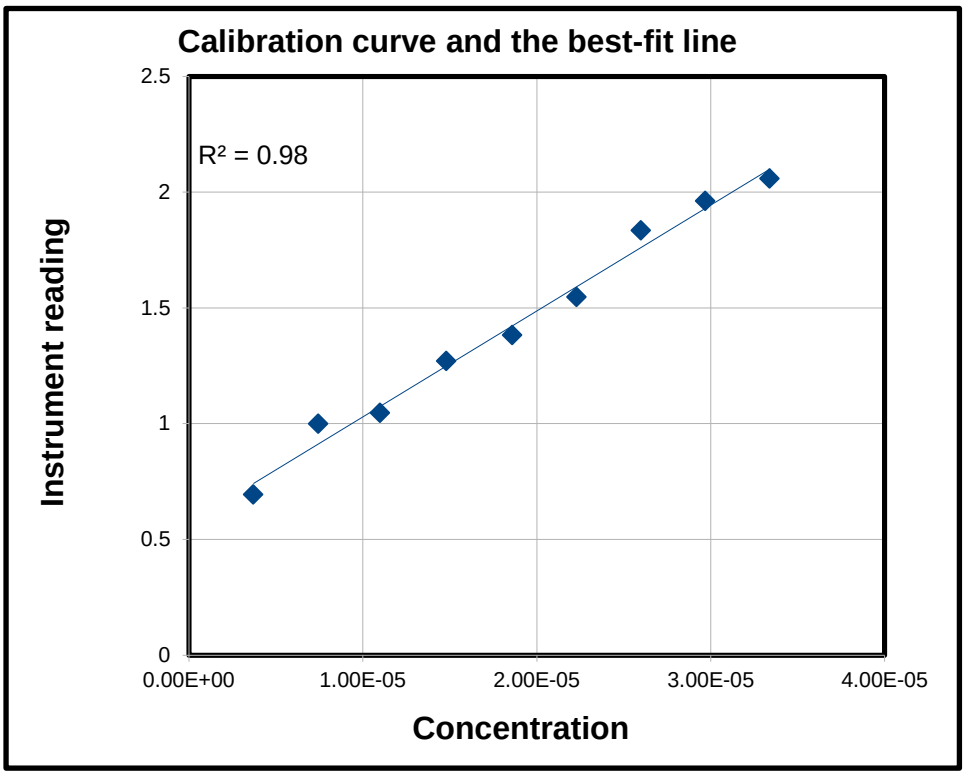

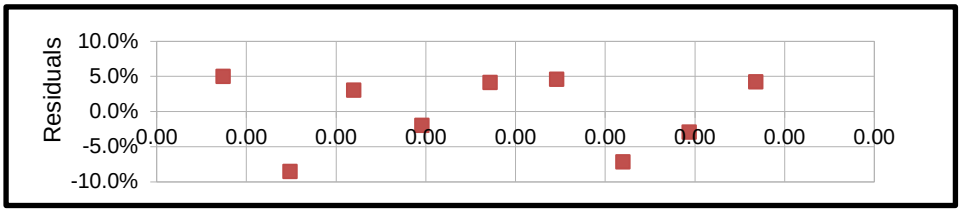

Standard deviation of the residuals = 13.5%

	Value	Error (σ)	% Error
Slope	2882.8421	178.9241	6.21%
Intercept	0.0257	0.0143	55.42%

Figure S40. Analytical calibration curve using a simple liner curve fit, with error estimation of H_2-TDtBHPP-MN (**3**) for fluoride addition.

Table S4. B3LYP/LANL2DZ calculated parameters for the investigated porphyrin and porphyrinogens for **3**.

compound	HOMO+1 (eV)	HOMO (eV)	LUMO (eV)	LUMO+1 (eV)	HOMO-LUMO gap (eV)
H_2-TDtBHPP	-5.932	-4.838	-2.285	-2.236	2.553
H_2-TDtBHPP-MN(**3**)	-5.708	-5.1209	-3.019	-2.563	2.1019
H_2-TDtBHPP-MN+ CN^- (**5**)	-3.2106	-1.977	-0.595	-0.565	1.382
H_2-TDtBHPP-MN+F^- (**4.F**$^-$)	-1.665	-1.521	0.467	0.558	1.988
H_2-TDtBHPP-MN+ F^-+ H_2O Wash (**4**)	-6.153	-5.865	-3.909	-3.555	1.956

Table S5. B3LYP/LANL2DZ calculated parameters for the investigated porphyrin and porphodimethene for **2**.

compound	HOMO+1 (eV)	HOMO (eV)	LUMO (eV)	LUMO+1 (eV)	HOMO-LUMO gap (eV)
Ni-TDtBHPP-CHO	-5.427	-5.029	-2.534	-2.309	2.495
Ni-TDtBHPP-MN(**2**)	-5.614	-5.225	-2.952	-2.467	2.273
Ni-TDtBHPP-MN + CN^-	-3.292	-1.852	-0.4291	-0.3782	1.423
Ni-TDtBHPP-MN + F^-	-6.026	-5.235	-4.227	-3.3217	1.008

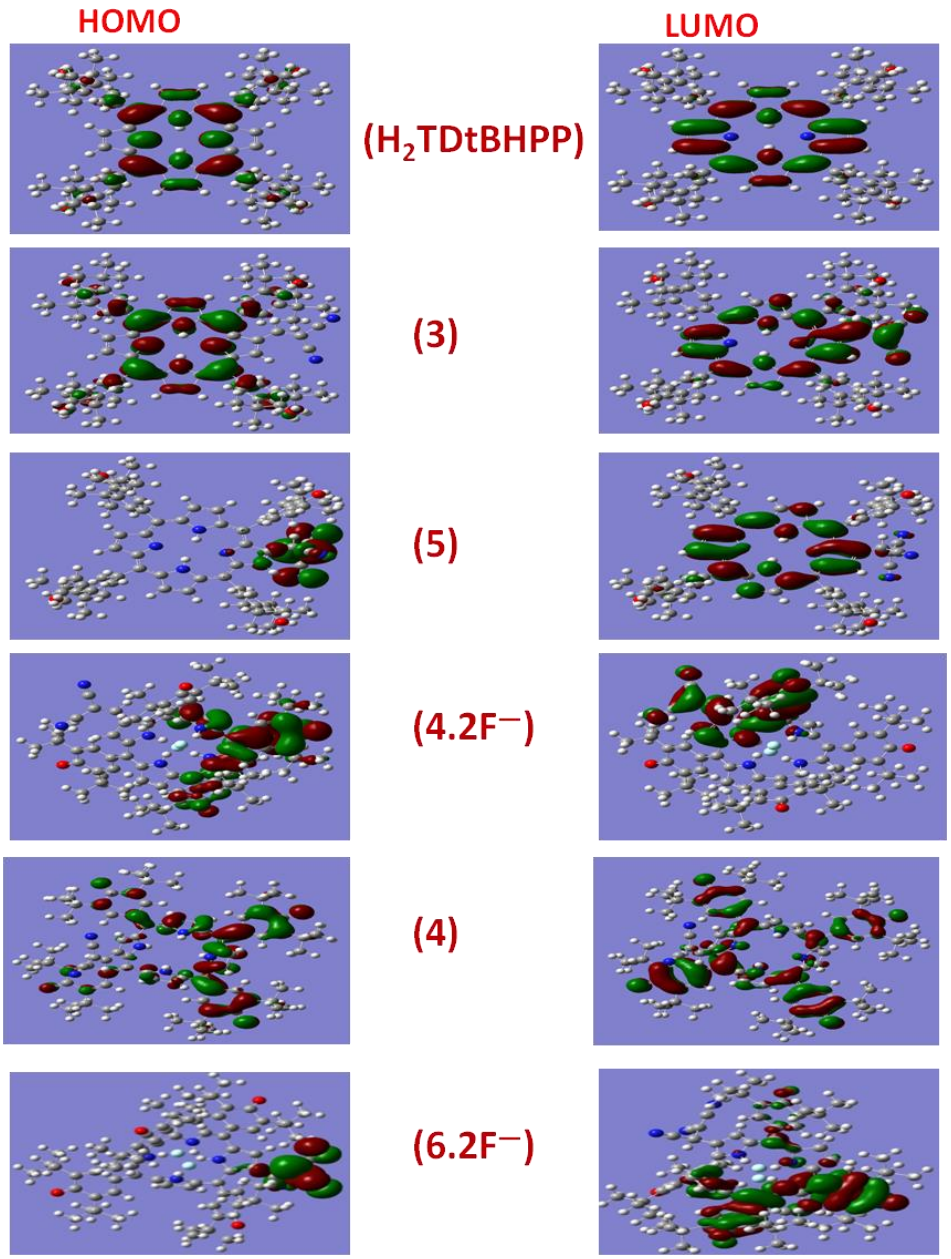

Figure S41. Coefficients of the first HOMO and the first LUMO for the optimized H_2-TDtBHPP, **3**, **5**, **4.2F**$^{-}$, **4** and **6.2F**$^{-}$.

Table S6. Tunable two-input/multi-output system for **1** using CN^- and F^- as inputs.

Memory element		λ_{max} 423 nm	λ_{max} 462 nm	λ_{max} 785 nm
INPUT 1 (CN^-)	INPUT 2 (F^-)			
0	0	"0"	"1"	"0"
1	0	"1"	"0"	"0"
0	1	"0"	"0"	"1"
1	1	"0"	"0"	"1"

Table S7. Tunable two-input/multi-output system for **2** using CN^- and F^- as inputs.

Memory element		λ_{max} 426 nm	λ_{max} 462 nm	λ_{max} 532 nm
INPUT 1 (CN^-)	INPUT 2 (F^-)			
0	0	"0"	"1"	"0"
1	0	"1"	"0"	"0"
0	1	"0"	"0"	"1"
1	1	"0"	"0"	"1"